

Phase diagram of QCD matter with magnetic field: domain-wall Skyrmion chain in chiral soliton lattice

Minoru Eto,^{a,b} Kentaro Nishimura^{c,d,b} and Muneto Nitta^{e,b,c}

^aDepartment of Physics, Yamagata University,

Kojirakawa-machi 1-4-12, Yamagata, Yamagata 990-8560, Japan

^bResearch and Education Center for Natural Sciences, Keio University,

4-1-1 Hiyoshi, Yokohama, Kanagawa 223-8521, Japan

^cInternational Institute for Sustainability with Knotted Chiral Meta Matter (SKCM²),

Hiroshima University, 1-3-2 Kagamiyama, Higashi-Hiroshima, Hiroshima 739-8511, Japan

^dKEK Theory Center, Tsukuba 305-0801, Japan

^eDepartment of Physics, Keio University, 4-1-1 Hiyoshi, Kanagawa 223-8521, Japan

E-mail: meto@sci.kj.yamagata-u.ac.jp, nishiken@post.kek.jp,

nitta@phys-h.keio.ac.jp

ABSTRACT: QCD matter in strong magnetic field exhibits a rich phase structure. In the presence of an external magnetic field, the chiral Lagrangian for two flavors is accompanied by the Wess-Zumino-Witten (WZW) term containing an anomalous coupling of the neutral pion π_0 to the magnetic field via the chiral anomaly. Due to this term, the ground state is inhomogeneous in the form of either chiral soliton lattice (CSL), an array of solitons in the direction of magnetic field, or domain-wall Skyrmion (DWSk) phase in which Skyrmions supported by $\pi_3[\text{SU}(2)] \simeq \mathbb{Z}$ appear inside the solitons as topological lumps supported by $\pi_2(S^2) \simeq \mathbb{Z}$ in the effective worldvolume theory of the soliton. In this paper, we determine the phase boundary between the CSL and DWSk phases beyond the single-soliton approximation, within the leading order of chiral perturbation theory. To this end, we explore a domain-wall Skyrmion chain in multiple soliton configurations. First, we construct the effective theory of the CSL by the moduli approximation, and obtain the $\mathbb{C}P^1$ model or $O(3)$ model, gauged by a background electromagnetic gauge field, with two kinds of topological terms coming from the WZW term: one is the topological lump charge in 2+1 dimensional worldvolume and the other is a topological term counting the soliton number. Topological lumps in the 2+1 dimensional worldvolume theory are superconducting rings and their sizes are constrained by the flux quantization condition. The negative energy condition of the lumps yields the phase boundary between the CSL and DWSk phases. We find that a large region inside the CSL is occupied by the DWSk phase, and that the CSL remains metastable in the DWSk phase in the vicinity of the phase boundary.

KEYWORDS: Phase Diagram or Equation of State, Chiral Lagrangian, Solitons Monopoles and Instantons

ARXIV EPRINT: [2311.01112](https://arxiv.org/abs/2311.01112)

Contents

1	Introduction	1
2	Chiral soliton lattice in strong magnetic field	4
3	Effective worldvolume theory of soliton in chiral soliton lattice	7
4	Domain-wall Skyrmion chain and domain-wall Skyrmion phase	10
5	Summary and discussion	14

1 Introduction

The determination of matter phases stands as a pivotal challenge in modern physics. Quantum Chromodynamics (QCD) serves as the foundational theory of strong interactions, encapsulating descriptions of quarks, gluons, and hadrons (both baryons and mesons) as bound states of the aforementioned entities. Remarkably, the lattice QCD offers a comprehensive description of these bound states. The QCD phase diagram, especially under extreme conditions like high baryon density, pronounced magnetic fields, and rapid rotation, garners significant attention [1]. Such conditions are not merely of theoretical interest but pertain to real-world scenarios like the interior of neutron stars and phenomena observed in heavy-ion collisions. While lattice QCD is adept at addressing scenarios with zero baryon density, its extension to finite baryon density is hampered by the infamous sign problem. Contrastingly, in situations where chiral symmetry undergoes spontaneous breaking, the emergence of massless Nambu-Goldstone (NG) bosons or pions, which are dominant at low energy, is observed. This low-energy dynamics is aptly described by either the chiral Lagrangian or the chiral perturbation theory (ChPT) centered on the pionic degree of freedom. Importantly, this description is predominantly dictated by symmetries and only modulated by certain constants, including the pion's decay constant f_π and quark masses m_π [2, 3].

As an extreme condition, QCD in strong magnetic fields has received quite intense attention because of the interior of neutron stars and heavy-ion collisions. In the presence of an external magnetic field, the chiral Lagrangian is accompanied by the Wess-Zumino-Witten (WZW) term containing an anomalous coupling of the neutral pion π_0 to the magnetic field via the chiral anomaly [4, 5] in terms of the Goldstone-Wilczek current [6, 7]. It was determined to reproduce the so-called chiral separation effect [1, 4, 8–10] in terms of the neutral pion π_0 . Then, at a finite baryon chemical potential μ_B under a sufficiently strong magnetic field B , if the inequality

$$B \geq B_{\text{CSL}} = \frac{16\pi m_\pi f_\pi^2}{e\mu_B}: \text{ the blue curve in figure 1} \quad (1.1)$$

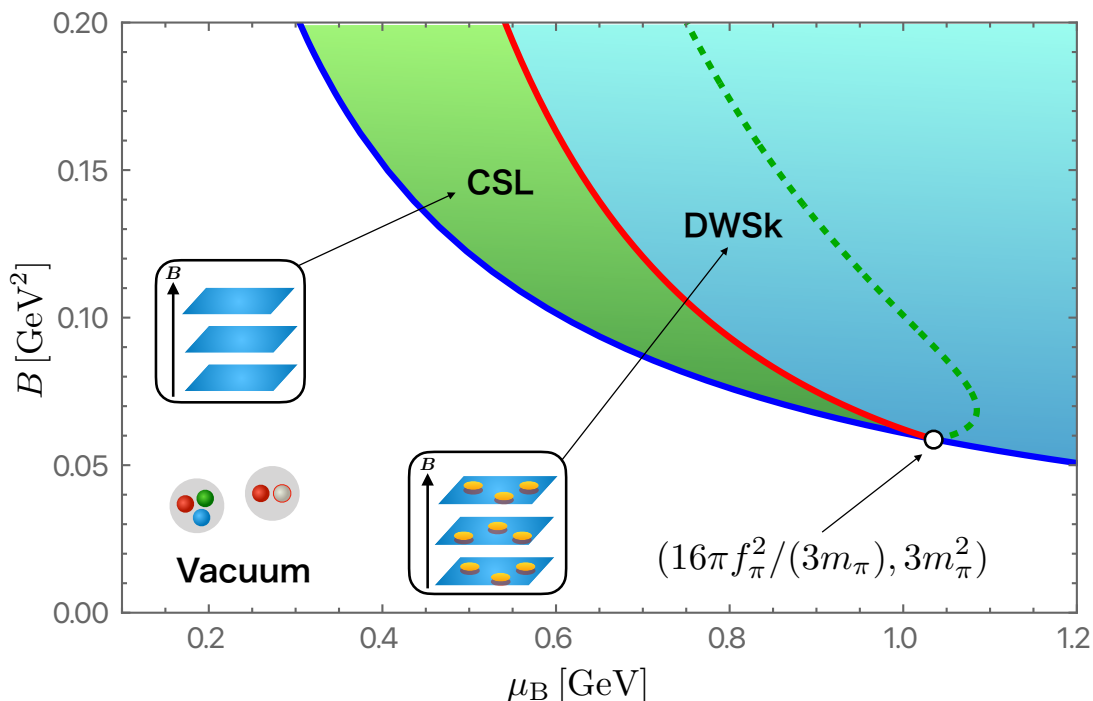


Figure 1. Phase diagram of QCD matter with magnetic fields. The blue curve denotes the boundary of QCD vacuum by Son and Stephanov in eq. (1.1). The green dotted curve denotes the instability curve of the CSL by the charged pion condensation in eq. (4.17), given below, that asymptotically reduces to eq. (1.2) for large B . The red curve is our new finding of the phase boundary between the CSL and DWSk phases in eq. (4.16), given below, that behaves asymptotically as eq. (4.20), given below. The blue, red and green dotted curves meet at the tricritical point in eq. (1.3). The CSL configuration is a metastable state in the region between the red and green dotted curves.

holds, the ground state of QCD with two flavors (up and down quarks) becomes inhomogeneous in the form of a chiral soliton lattice (CSL) consisting of a stack of domain walls or solitons carrying a baryon number [5, 11, 12].¹ A possibility of an experimental detection of inhomogeneous states including the CSL has been proposed in ref. [13].

However, Brauner and Yamamoto found that such a CSL state is unstable against a charged pion condensation in a region of higher density and/or stronger magnetic field [12]. The asymptotic expression of the instability curve at large B is

$$B_{\text{CPC}} \sim \frac{16\pi^4 f_\pi^4}{\mu_B^2}: \text{ the green dotted curve (at large } B \text{) in figure 1} \quad (1.2)$$

above which the CSL is unstable, where ‘‘CPC’’ denotes the charged pion condensation. The full expression of the boundary is given in eq. (4.17), below, and is denoted by the green dotted curve in figure 1. In ref. [29], an Abrikosov’s vortex lattice was proposed as a

¹CSLs manifest in diverse scenarios within QCD. Examples include situations under rapid rotation [14–18] and due to thermal fluctuations [19–22]. Investigations into the quantum nucleation of CSLs can be found in [23, 24], and discussions on quasicrystals are provided in [25]. The potential interplay between Skyrmion crystals at zero magnetic field and the CSL phase has been explored in refs. [26–28].

consequence of the charged pion condensation (see also a recent paper [30]). This instability curve ends at the tricritical point:

$$\begin{aligned}
 (\mu_c, B_c) &= \left(\frac{16\pi f_\pi^2}{3m_\pi}, \frac{3m_\pi^2}{e} \right) \\
 &\approx (1.03 \text{ GeV}, 0.06\text{GeV}^2 \sim 1.0 \times 10^{19}\text{G}) : \text{ the white dot in figure 1,} \quad (1.3)
 \end{aligned}$$

with the vacuum values of the physical quantities $f_\pi \approx 93 \text{ MeV}$ and $m_\pi \approx 140 \text{ MeV}$.

In our previous paper [31], we proposed that there is the domain-wall Skyrmion (DWSk) phase in the region inside the CSL,

$$\mu_B \geq \mu_c \quad (1.4)$$

with μ_c in eq. (1.3), in which Skyrmions are created on top of the solitons in the ground state. To show this, the effective world-volume theory on a single soliton was constructed as an $O(3)$ sigma model or the CP^1 model with topological terms induced from the WZW term. Then, there appear topological lumps (or baby Skyrmions) supported by $\pi_2(CP^1) \simeq \mathbb{Z}$ on the world volume, corresponding to 3+1 dimensional Skyrmions supported by $\pi_3[SU(2)] \simeq \mathbb{Z}$ in the bulk point of view. Such a composite state of a domain wall and Skyrmions are called domain-wall Skyrmions.² However, we used a single-soliton approximation, considering the domain-wall Skyrmion on a single soliton [31]. In other words, we assumed that the solitons are well separated, and this assumption can be justified only at the phase boundary between the QCD vacuum and the CSL phase in eq. (1.1), namely at the tricritical point in eq. (1.3). On the other hand, the instability curve of the CSL due to a charged pion condensation also ends at the same point in eq. (1.3) [12]. Therefore, a natural question that arises is the compatibility between the DWSk phase and instability curve.

In this paper, we determine the phase boundary between the CSL and DWSk phases beyond the single-soliton approximation, in which the boundary was the straight vertical line in eq. (1.4) ending on the tricritical point represented by the white dot in figure 1. To this end, we explore domain-wall Skyrmion chains in multiple soliton configurations. A similar domain-wall skyrmion chain has been also studied in chiral magnets [45]. As is well known, the CSL configuration is analytically given by the elliptic function. We construct the effective theory of the CSL by the moduli approximation [52–54], in which we promote the CP^1 moduli of the CSL to fields depending on the worldvolume (x^0, x^1, x^2) and integrate over one period of the lattice in the codimensional direction x^3 . We obtain the CP^1 model or $O(3)$ model with two kinds of topological terms coming from the WZW term: one is topological lump charge responsible for $\pi_2(S^2) \simeq \mathbb{Z}$ in 2+1 dimensional worldvolume and the other is a topological term counting the soliton number. We then construct lumps in the 2+1 dimensional worldvolume theory. Since the electromagnetic $U(1)$ gauge symmetry

²Domain-wall Skyrmions were initially introduced in the context of field theory, both in 3+1 dimensions [32–37] and in 2+1 dimensions [38–40]. In the realm of condensed matter physics, the 2+1 dimensional variant has been both theoretically investigated [41–48] and experimentally observed in chiral magnets [49, 50]. The term “domain-wall Skyrmions” can be traced back to its initial use in ref. [51], where it described Yang-Mills instantons situated within a domain wall in 4+1 dimensions. In this setting, these entities are represented as Skyrmions in the effective 3+1 dimensional domain-wall theory. However, a more appropriate designation for them might be “domain-wall instantons”.

is spontaneously broken around a ring surrounding the lump, the lump can be regarded as a superconducting ring. Then its size modulus is fixed by the flux quantization condition of the superconducting ring, enhancing its stability. The lumps in the soliton worldvolume correspond to Skyrmions in the bulk, Skyrmions periodically sit on each soliton in the CSL, and thus the configuration is a domain-wall Skyrmion chain. The condition that a lump has negative energy yields the phase boundary between the CSL and DWSk phases denoted by the red curve in figure 1. In the strong magnetic field limit, the phase boundary asymptotically behaves as

$$B_c \sim \frac{4\pi^3 f_\pi^4}{\mu_B^2} = \frac{1}{4\pi} B_{\text{CPC}}. \tag{1.5}$$

The important is that the boundary curve has the lower critical chemical potential μ_B and lower critical magnetic field B than those of the instability curve (the green dotted curve in figure 1) of the CSL in eq. (1.2). Therefore, the CSL state remains metastable in the region between the red and green dotted curves.

This paper is organized as follows. In section 2 we present a CSL in the strong magnetic field. In section 3 we construct the effective worldvolume theory of a one period of the CSL, by the moduli approximation. In section 4 we construct topological lumps in the soliton's worldvolume theory and determine the phase boundary between the CSL and DWSk phases. Section 5 is devoted to a summary and discussion.

2 Chiral soliton lattice in strong magnetic field

We focus on the phase where chiral symmetry is spontaneously broken. The effective field theory of pions, known as ChPT, can describe the low-energy dynamics. The pion fields are represented by a 2×2 unitary matrix,

$$\Sigma = e^{i\tau_a \chi_a}, \tag{2.1}$$

where τ_a (with $a = 1, 2, 3$) are the Pauli matrices, normalized as $\text{tr}(\tau_a \tau_b) = 2\delta_{ab}$. The field Σ transforms under $SU(2)_L \times SU(2)_R$ chiral symmetry as

$$\Sigma \rightarrow L\Sigma R^\dagger, \tag{2.2}$$

where both L and R are 2×2 unitary matrices. Then, the effective Lagrangian at the $\mathcal{O}(p^2)$ order is ($\mu = 0, \dots, 3$)

$$\mathcal{L}_{\text{ChPT}} = \frac{f_\pi^2}{4} \text{tr} \left(D_\mu \Sigma D^\mu \Sigma^\dagger \right) - \frac{f_\pi^2 m_\pi^2}{4} \text{tr} \left(2\mathbf{1} - \Sigma - \Sigma^\dagger \right), \tag{2.3}$$

where f_π and m_π are pion's decay constant and mass, respectively, and D_μ is a covariant derivative defined by

$$D_\mu \Sigma \equiv \partial_\mu \Sigma + ie A_\mu [Q, \Sigma], \tag{2.4}$$

$$Q = \frac{1}{6} \mathbf{1} + \frac{1}{2} \tau_3. \tag{2.5}$$

where Q is a matrix of the electric charge of quarks. The $U(1)_{\text{EM}}$ transformation is given by

$$\Sigma \rightarrow e^{i\lambda \frac{\tau_3}{2}} \Sigma e^{-i\lambda \frac{\tau_3}{2}} \quad \text{and} \quad A_\mu \rightarrow A_\mu - \frac{1}{e} \partial_\mu \lambda. \quad (2.6)$$

The external $U(1)_B$ gauge field A_μ^B can couple to Σ via the Goldstone-Wilczek current [6, 7]. The conserved and gauge-invariant baryon current in the external magnetic field is detailed in refs. [5, 6]:

$$j_{\text{GW}}^\mu = -\frac{\epsilon^{\mu\nu\alpha\beta}}{24\pi^2} \text{tr} (L_\nu L_\alpha L_\beta - 3ie\partial_\nu [A_\alpha Q(L_\beta + R_\beta)]) , \quad (2.7)$$

with $A_\mu^B = (\mu_B, \mathbf{0})$, and introducing the notations $L_\mu \equiv \Sigma \partial_\mu \Sigma^\dagger$ and $R_\mu \equiv \partial_\mu \Sigma^\dagger \Sigma$.

The effective Lagrangian that couples to A_μ^B is expressed as

$$\mathcal{L}_{\text{WZW}} = -A_\mu^B j_{\text{GW}}^\mu, \quad (2.8)$$

which is recognized as the WZW term [4, 5]. Thus, the total Lagrangian is

$$\mathcal{L} = \mathcal{L}_{\text{ChPT}} + \mathcal{L}_{\text{WZW}}. \quad (2.9)$$

An important observation is warranted at this point. In order to formulate an effective Lagrangian, we adopt a modification of the standard power counting scheme of ChPT as presented in ref. [21]:

$$\partial_\mu, m_\pi, A_\mu = \mathcal{O}(p^1), \quad A_\mu^B = \mathcal{O}(p^{-1}). \quad (2.10)$$

In this power-counting scheme, eq. (2.8) is of order $\mathcal{O}(p^2)$ and is consistent with eq. (2.3). It is significant to note that μ_B only manifests in the WZW term of eq. (2.8), which allows us to attribute a negative power counting to μ_B . The effective field theory up to $\mathcal{O}(p^2)$ must incorporate both terms in eq. (2.7). However, previous studies on the CSLs have not taken into account the first term in eq. (2.7).

We emphasize that the inclusion of an $\mathcal{O}(p^4)$ term, such as the Skyrme term and the chiral anomaly term (which includes $\pi_0 \mathbf{E} \cdot \mathbf{B}$), is not essential for our results. As a result, our analysis maintains its model-independence. Moreover, it should be noted that at the leading order, the gauge field is nondynamical due to its kinetic term being of order $\mathcal{O}(p^4)$.

We note that our effective theory admits a parallel stack of the sine-Gordon soliton expanding perpendicular to the external magnetic field, which is called the chiral soliton lattice. This state is stable under a sufficiently large magnetic field, as shown in [5]. If we consider the case of no charged pions $\Sigma_0 = e^{i\tau_3 \chi_3}$, the effective Lagrangian reduces to

$$\mathcal{L} = \frac{f_\pi^2}{2} (\partial_\mu \chi_3)^2 - f_\pi^2 m_\pi^2 (1 - \cos \chi_3) + \frac{e\mu_B}{4\pi^2} \mathbf{B} \cdot \nabla \chi_3. \quad (2.11)$$

The ordinary QCD vacuum corresponds to $\chi_3 = 0$. However, the third term in eq. (2.11) modifies the ground state of QCD at finite μ_B and \mathbf{B} . The anticipated time-independent neutral pion background χ_3 is obtained by minimization of the energy functional. The static Hamiltonian depending only on the z coordinate is given by

$$\mathcal{H} = \frac{f_\pi^2}{2} (\partial_z \chi_3)^2 + f_\pi^2 m_\pi^2 (1 - \cos \chi_3) - \frac{e\mu_B B}{4\pi^2} \partial_z \chi_3. \quad (2.12)$$

Without loss of generality, we will orient the uniform external magnetic field along the z -axis; $\mathbf{B} = (0, 0, B)$. We note that eq. (2.12) have the first derivative term proportional to $\partial_z \chi_3$. Then, the configuration of the ground state will have a nontrivial z -dependence. In order to determine the static configuration of χ_3 , let us solve the EOM of eq. (2.11). The equation of motion for such a one-dimensional configuration $\chi_3(z)$ then reads

$$\partial_z^2 \chi_3 = m_\pi^2 \sin \chi_3, \quad (2.13)$$

which can be analytically solved by the elliptic functions:

$$\chi_3^{\text{CSL}} = 2 \text{am} \left(\frac{m_\pi z}{\kappa}, \kappa \right) + \pi, \quad (2.14)$$

with a real constant κ ($0 \leq \kappa \leq 1$) called the elliptic modulus. This solution is a lattice state of the π_0 ($= f_\pi \chi_3$) meson with a period ℓ . The period ℓ satisfies the following equations:

$$\chi_3^{\text{CSL}}(z + \ell) = \chi_3^{\text{CSL}}(z) + 2\pi, \quad (2.15)$$

$$\ell = \frac{2\kappa K(\kappa)}{m_\pi}, \quad (2.16)$$

with the complete elliptic integral of the first kind $K(\kappa)$. Substituting eq. (2.14) into eq. (2.12) and integrating it between one period ℓ , we get the tension of a single soliton inside the CSL, that is the energy density per unit area integrated over one period

$$\mathcal{E} = \int_0^\ell dz \mathcal{H} = 4m_\pi f_\pi^2 \left[\frac{2E(\kappa)}{\kappa} + \left(\kappa - \frac{1}{\kappa} \right) K(\kappa) \right], \quad (2.17)$$

with the complete elliptic integral of the second kind $E(\kappa)$. Minimizing the energy density per unit length \mathcal{E}/ℓ with respect to k gives me the following condition:

$$\frac{E(\kappa)}{\kappa} = \frac{e\mu_B B}{16\pi m_\pi f_\pi^2}. \quad (2.18)$$

Since the left-hand side of eq. (2.18) is bounded from below as $E(\kappa)/\kappa \geq 1$ ($0 \leq \kappa \leq 1$), the CSL solution exists if and only if the following condition is satisfied [5, 12]:

$$B_{\text{CSL}} = \frac{16\pi m_\pi f_\pi^2}{e\mu_B}, \quad (2.19)$$

denoted by the blue curve in figure 1. Inserting the minimization condition (2.18) into eq. (2.17), we evaluate the energy density at the optimized k as:

$$\mathcal{E} = 4m_\pi f_\pi^2 \left(\kappa - \frac{1}{\kappa} \right) K(\kappa) < 0, \quad (2.20)$$

which is lower than that of the QCD vacuum. Therefore, the CSL is energetically more stable than the QCD vacuum.

3 Effective worldvolume theory of soliton in chiral soliton lattice

The preceding section concentrated exclusively on the π_0 meson. General solutions that encompass charged pions can be derived from Σ_0 through an $SU(2)_V$ transformation,

$$\Sigma = g\Sigma_0g^\dagger = \exp(i\chi_3^{\text{CSL}}g\tau_3g^\dagger), \quad (3.1)$$

where g represents an $SU(2)$ matrix. It is clear that Σ_0 is invariant under $SU(2)_V$ when $g = e^{i\tau_3\theta}$. Consequently, each soliton possesses moduli originated from the spontaneous symmetry breaking $SU(2)_V \rightarrow U(1)_3$ in the vicinity of the soliton:

$$\mathcal{M} \cong \frac{SU(2)_V}{U(1)_3} \cong \mathbb{C}P^1 \cong S^2. \quad (3.2)$$

Such a sine-Gordon soliton carrying non-Abelian $\mathbb{C}P^1$ moduli is called a non-Abelian sine-Gordon soliton [36, 55] (see also refs. [37, 56, 57]). However, unlike these references, our solitons are nontopological because they are not protected by topology and are rather stabilized by the WZW term.

For subsequent discussions, we characterize the $\mathbb{C}P^1$ moduli using the homogeneous coordinates $\phi \in \mathbb{C}^2$ of $\mathbb{C}P^1$, which fulfill the relations [36]

$$\phi^\dagger\phi = 1, \quad g\tau_3g^\dagger = 2\phi\phi^\dagger - \mathbf{1}_2. \quad (3.3)$$

In the context of ϕ , eq. (3.1) can be recast as

$$\Sigma = \exp(2i\chi_3^{\text{CSL}}\phi\phi^\dagger)u^{-1} = [\mathbf{1}_2 + (u^2 - 1)\phi\phi^\dagger]u^{-1}, \quad (3.4)$$

$$u \equiv e^{i\chi_3^{\text{CSL}}} = \exp\left(2i \operatorname{am}\left(\frac{m_\pi z}{\kappa}, \kappa\right) + \pi i\right). \quad (3.5)$$

Given that the moduli space is S^2 , we can also employ the real three-component vector \mathbf{n} defined as

$$\mathbf{n}_a = \phi^\dagger\tau_a\phi, \quad (3.6)$$

to describe this space. The π^0 CSL in eq. (2.14) corresponds to $n_3 = 1$.

Let us construct the low-energy effective field theory of the CSL based on the moduli approximation [52–54]. In the following, we will promote the moduli parameter ϕ as the fields on the 2 + 1-dimensional soliton's world volume. We first calculate the effective action coming from eq. (2.3). Substituting eq. (3.4) into eq. (2.3), we get

$$\begin{aligned} \mathcal{L}_{\text{ChPT}} = & \frac{f_\pi^2}{2}|1 - u^2|^2[(\phi^\dagger\partial_\alpha\phi)^2 + \partial_\alpha\phi^\dagger\partial^\alpha\phi] \\ & + \frac{e}{2}f_\pi^2A^\alpha|u^2 - 1|^2\left[\phi^\dagger\tau_3\phi \cdot \phi^\dagger\partial_\alpha\phi + \frac{1}{2}(\partial_\alpha\phi^\dagger\tau_3\phi - \phi^\dagger\tau_3\partial_\alpha\phi)\right] \\ & - \frac{e^2f_\pi^2}{8}A^2|u^2 - 1|^2\left[-1 + (\phi^\dagger\tau_3\phi)^2\right] \\ & - \frac{f_\pi^2}{2}(\partial_z\chi_3^{\text{CSL}})^2 - f_\pi^2m_\pi^2(1 - \cos\chi_3^{\text{CSL}}), \end{aligned} \quad (3.7)$$

where x^α ($\alpha = 0, 1, 2$) are world-volume coordinates. Integrating over z , the effective action stemming from eq. (3.7) can be calculated as

$$\int dz \mathcal{L}_{\text{ChPT}} = \mathcal{C}(\kappa)[(\phi^\dagger D_\alpha \phi)^2 + D_\alpha \phi^\dagger D^\alpha \phi] - \mathcal{E}, \quad (3.8)$$

with the Kähler class $\mathcal{C}(\kappa)$ defined by

$$\mathcal{C}(\kappa) \equiv \frac{16f_\pi^2 (2 - \kappa^2)E(\kappa) - 2(1 - \kappa^2)K(\kappa)}{3m_\pi \kappa^3} \quad (3.9)$$

and the tension \mathcal{E} of a single soliton in eq. (2.17), where we have used the integrals,

$$\int_0^{\frac{2\kappa K(\kappa)}{m_\pi}} dz |1 - u^2|^2 = \frac{16}{3m_\pi} \frac{2(2 - \kappa^2)E(\kappa) - 4(1 - \kappa^2)K(\kappa)}{\kappa^3}, \quad (3.10)$$

and the contribution of the gauge field can be summarized into the covariant derivative:

$$D_\alpha \phi = \left(\partial_\alpha + ieA_\alpha \frac{\tau_3}{2} \right) \phi. \quad (3.11)$$

The first term in eq. (3.8) is the kinetic term of ϕ , being equivalent to the gauged $\mathbb{C}P^1$ model. The second term in eq. (3.8) is the minus tension of each soliton, that is the energy density of the CSL in one period ℓ .

We next calculate the effective action coming from the WZW term in eq. (2.8). The contribution of the first term in eq. (2.7) to the WZW term in eq. (2.8) can be expressed as $\mu_B \mathcal{B}$. Here, we refer to the Skyrmoion charge density as

$$\mathcal{B} = \frac{-1}{24\pi^2} \epsilon^{ijk} \text{tr}(L_i L_j L_k), \quad (3.12)$$

which can be factorized as

$$\mathcal{B} = -\frac{1}{2\pi} (u - u^{-1})^2 \partial_z \chi_3^{\text{CSL}} q(x, y), \quad (3.13)$$

where the $\mathbb{C}P^1$ lump topological charge density is defined as

$$q(x, y) \equiv -\frac{i}{2\pi} \epsilon^{ij} \partial_i \phi^\dagger \partial_j \phi = \frac{1}{8\pi} \epsilon^{ij} \mathbf{n} \cdot (\partial_i \mathbf{n} \times \partial_j \mathbf{n}). \quad (3.14)$$

Integration of q over x and y gives the quantized lump charge k , being associated with $\pi_2(\mathbb{C}P^1)$:

$$k \equiv \int d^2x q \in \pi_2(\mathbb{C}P^1) \simeq \mathbb{Z}. \quad (3.15)$$

Integrating \mathcal{B} from 0 to ℓ , we get

$$\int_0^\ell dz \mathcal{B} = 2q(x, y), \quad (3.16)$$

where we have used

$$-\int_0^\ell dz \frac{1}{2\pi} (u - u^{-1})^2 \partial_z \chi_3^{\text{CSL}} = \frac{16}{\pi} \int_0^{2K(\kappa)} d\bar{z} \text{sn}(\bar{z}, \kappa)^2 \text{cn}(\bar{z}, \kappa)^2 \text{dn}(\bar{z}, \kappa) = 2. \quad (3.17)$$

Integrating eq. (3.16) over the xy plane, we find the baryon number b per one period:

$$b = 2k \in \pi_3[\text{SU}(2)]. \quad (3.18)$$

We thus have seen that one lump on one soliton corresponds to two Skyrmions (baryons) in the bulk. This one-to-two correspondence is in contrast to the domain-wall Skyrmions in QCD under rapid rotation [18], in which case one lump on a soliton corresponds to one Skyrmion.

The contribution of the second term in eq. (2.7) to the WZW term in eq. (2.8) can be divided into two terms as follows:

$$\begin{aligned} \frac{i e \mu_B}{16 \pi^2} \epsilon^{0ijk} \partial_i [A_j \text{tr}(\tau_3 L_k + \tau_3 R_k)] &= \frac{i e \mu_B}{16 \pi^2} \epsilon^{0ijk} \partial_i A_j \text{tr}(\tau_3 L_k + \tau_3 R_k) \\ &+ \frac{i e \mu_B}{16 \pi^2} \epsilon^{0ijk} A_j \text{tr} \tau_3 (\partial_i \Sigma \partial_k \Sigma^\dagger + \partial_k \Sigma^\dagger \partial_i \Sigma). \end{aligned} \quad (3.19)$$

We consider the uniform external magnetic field along the z -axis, $\mathbf{B} = (0, 0, B)$. Then, the first term in eq. (3.19) becomes

$$-\frac{i e \mu_B}{16 \pi^2} B \text{tr} \tau_3 (L_3 + R_3). \quad (3.20)$$

In terms of the projection operator $P \equiv \phi \phi^\dagger$ satisfying $P^2 = P$, R_k and L_k can be expressed as

$$L_k = (1 - 2P) i \partial_k \chi_3^{\text{CSL}} + (u^{-2} - 1) \partial_k P + |u^2 - 1|^2 P \partial_k P, \quad (3.21)$$

$$R_k = (1 - 2P) i \partial_k \chi_3^{\text{CSL}} + (u^{-2} - 1) \partial_k P + |u^2 - 1|^2 \partial_k P \cdot P. \quad (3.22)$$

Since ϕ does not depend on z , the second and third terms in L_3 and R_3 vanish. Therefore, eq. (3.20) becomes

$$-\frac{e \mu_B B}{4 \pi^2} (\phi^\dagger \tau_3 \phi) \partial_3 \chi_3^{\text{CSL}}, \quad (3.23)$$

and integrating over z , we get

$$\int_0^\ell dz \frac{i e \mu_B}{16 \pi^2} \epsilon^{0ijk} \partial_i A_j \text{tr}(\tau_3 L_k + \tau_3 R_k) = -\frac{e \mu_B B}{2 \pi} \phi^\dagger \tau_3 \phi, \quad (3.24)$$

where we have used the boundary condition of χ_3^{CSL} for a single soliton, $\chi_3^{\text{CSL}}(\ell) - \chi_3^{\text{CSL}}(0) = 2\pi$. We next calculate the second term in eq. (3.19). Substituting eq. (3.4) into $\partial_i \Sigma \partial_k \Sigma^\dagger$ and $\partial_k \Sigma^\dagger \partial_i \Sigma$, these two quantities can be calculated as

$$\begin{aligned} \partial_i \Sigma \partial_k \Sigma^\dagger &= [(1 - u^{-2}) - (u^2 - u^{-2})P] i \partial_i \chi_3^{\text{CSL}} \partial_k P \\ &- [(1 - u^2) + (u^2 - u^{-2})P] i \partial_k \chi_3^{\text{CSL}} \partial_i P + |1 - u^2|^2 \partial_i P \partial_k P, \end{aligned} \quad (3.25)$$

$$\begin{aligned} \partial_k \Sigma^\dagger \partial_i \Sigma &= [(1 - u^{-2}) - (u^2 - u^{-2})P] i \partial_i \chi_3^{\text{CSL}} \partial_k P \\ &- [(1 - u^2) + (u^2 - u^{-2})P] i \partial_k \chi_3^{\text{CSL}} \partial_i P + |1 - u^2|^2 \partial_k P \partial_i P. \end{aligned} \quad (3.26)$$

Hence, we can represent $\epsilon^{0ijk} \text{tr}(\partial_i \Sigma \partial_k \Sigma^\dagger + \partial_k \Sigma^\dagger \partial_i \Sigma)$ in terms of u and ϕ as follows:

$$\begin{aligned}
 & \epsilon^{0ijk} \text{tr} \tau_3 (\partial_i \Sigma \partial_k \Sigma^\dagger + \partial_k \Sigma^\dagger \partial_i \Sigma) \\
 &= \epsilon^{0ijk} \text{tr} \tau_3 \left\{ 2i \left[-1 + (1 + u^2) P \right] (u^{-2} - 1) \partial_i \chi_3^{\text{CSL}} \partial_k P \right. \\
 &\quad \left. + 2i \left[-1 + (1 + u^{-2}) P \right] (u^2 - 1) \partial_i \chi_3^{\text{CSL}} \partial_k P \right\} \\
 &= 2i |1 - u^2|^2 \epsilon^{0ijk} \partial_i \chi_3^{\text{CSL}} \text{tr} \tau_3 \partial_k P \\
 &= 2i |1 - u^2|^2 \epsilon^{03jk} \partial_3 \chi_3^{\text{CSL}} \text{tr} \tau_3 \partial_k P.
 \end{aligned} \tag{3.27}$$

Inserting this expression into the second term in eq. (3.19), it becomes

$$-\frac{e\mu_B}{8\pi^2} \epsilon^{03jk} |1 - u^2|^2 \partial_3 \chi_3^{\text{CSL}} A_j \partial_k (\phi^\dagger \tau_3 \phi). \tag{3.28}$$

Integrating over z , we get

$$\int_0^\ell dz \frac{i e \mu_B}{16\pi^2} \epsilon^{0ijk} A_j \text{tr} \tau_3 (\partial_i \Sigma \partial_k \Sigma^\dagger + \partial_k \Sigma^\dagger \partial_i \Sigma) = -\frac{e\mu_B}{2\pi} \epsilon^{03jk} A_j \partial_k (\phi^\dagger \tau_3 \phi), \tag{3.29}$$

where we have used the integral eq. (3.17). Summing up eqs. (3.24) and (3.29), the effective Lagrangian from the second term in eq. (2.7) can be calculated as

$$-\frac{e\mu_B}{2\pi} \epsilon^{03jk} \partial_j (A_k \phi^\dagger \tau_3 \phi). \tag{3.30}$$

Finally, we arrive at the effective Lagrangian of the non-Abelian sine-Gordon soliton under the magnetic field:

$$\begin{aligned}
 \mathcal{L}_{\text{DW}} &\equiv \int_0^\ell dz (\mathcal{L}_{\text{ChPT}} + \mathcal{L}_{\text{WZW}}) \\
 &= -\left(\mathcal{E} - \frac{e\mu_B B}{2\pi} \right) + \mathcal{C}(\kappa) [(\phi^\dagger D_\alpha \phi)^2 + D_\alpha \phi^\dagger D^\alpha \phi] \\
 &\quad + 2\mu_B q + \frac{e\mu_B}{2\pi} \epsilon^{03jk} \partial_j [A_k (1 - n_3)].
 \end{aligned} \tag{3.31}$$

This is a background-gauged $\mathbb{C}P^1$ model or $O(3)$ model with the topological terms. Note that in the single-soliton limit ($\kappa = 1$), the Kähler class in eq. (3.9) reduces to $\mathcal{C}(\kappa = 1) = 16f_\pi^2/3m_\pi^2$ recovering our previously result [31].

4 Domain-wall Skyrmion chain and domain-wall Skyrmion phase

We examine Skyrmions within the domain-wall effective theory described by eq. (3.31). Initially, we neglect the gauge coupling by setting $D_\mu \rightarrow \partial_\mu$, considering the effects of the WZW term from eqs. (2.7) and (2.8). Subsequently, we incorporate the effects of the gauge coupling. The resulting static Hamiltonian is given by

$$\mathcal{H}_{\text{DW}} = \frac{\mathcal{C}(\kappa)}{4} \partial_i \mathbf{n} \cdot \partial_i \mathbf{n} - 2\mu_B q - \frac{e\mu_B}{2\pi} \epsilon^{03jk} \partial_j [A_k (1 - n_3)]. \tag{4.1}$$

Since the constants in eq. (3.31) only give the condition of whether the domain wall appears or not, it is sufficient to consider $B > B_c$, and thus have been omitted in eq. (4.1). Then, the total energy $E_{\text{DW}} = \int d^2x \mathcal{H}_{\text{DW}}$ is bounded from below as

$$E_{\text{DW}} \geq 2\pi\mathcal{C}(\kappa)|k| - 2\mu_B k - \frac{e\mu_B}{2\pi} \int d^2x \epsilon^{03jk} \partial_j [A_k(1 - n_3)], \quad (4.2)$$

which is called the Bogomol'nyi bound, where we have used

$$\partial_i \mathbf{n} \cdot \partial_i \mathbf{n} = \frac{1}{2} (\partial_i \mathbf{n} \pm \epsilon_{ij} \mathbf{n} \times \partial_j \mathbf{n})^2 \pm 8\pi q. \quad (4.3)$$

The inequality in eq. (4.2) is saturated only when the fields satisfy the (anti-)Bogomol'nyi-Prasad-Sommerfield (BPS) equation [58]

$$\partial_i \mathbf{n} \pm \epsilon_{ij} \mathbf{n} \times \partial_j \mathbf{n} = 0, \quad (4.4)$$

where the upper (lower) sign corresponds to the (anti-)BPS equation. It is interesting to observe that the second term in eq. (4.1) splits energies between BPS lumps $k > 0$ and anti-BPS lumps $k < 0$.³ The BPS solutions to this equation characterized by the winding number k (> 0) is given by [58]

$$n_3 = \frac{1 - |f|^2}{1 + |f|^2}, \quad f = \frac{b_{k-1} w^{k-1} + \dots + b_0}{w^k + a_{k-1} w^{k-1} + \dots + a_0}, \quad (4.5)$$

where $w \equiv x + iy$, and the set of complex parameters $\{a_A, b_A\}$ ($A = 0, 1, \dots, k-1$) are the moduli parameters.

We examine the gauge coupling between \mathbf{n} and A_α . With the electromagnetic gauge symmetry $U(1)_{\text{EM}}$ generated by τ_3 , the transformation of $n_1 + in_2$ is given by

$$n_1 + in_2 \rightarrow e^{-i\lambda}(n_1 + in_2), \quad (4.6)$$

while n_3 remains neutral. The covariant derivative is

$$D_\alpha(n_1 + in_2) = (\partial_\alpha - ieA_\alpha)(n_1 + in_2). \quad (4.7)$$

Let C be a closed curve where $n_3 = 0$ and D its interior. Due to the spontaneous breaking of $U(1)_{\text{EM}}$ symmetry around $|n_1 + in_2| = 1$, curve C functions as a superconducting loop, carrying a persistent current. Expressing $n_1 + in_2 = e^{i\psi}$ on C , the gauge field configuration along C is determined by the gradient energy minimization, leading to $|D_\alpha(n_1 + in_2)|^2 = 0$ and $\partial_\alpha \psi = eA_\alpha$. Consequently, the flux and area quantization on D becomes

$$BS_D = \int_D d^2x B = \oint_C dx^i A_i = \frac{1}{e} \oint_C dx^i \partial_i \psi = \frac{2\pi k}{e}, \quad (4.8)$$

where k is the lump number on D and S_D is the area of D .

³This situation is analogous to magnetic Skyrmions in chiral magnets (see, e.g. ref. [59]), in which case the so-called Dzyaloshinskii-Moriya interaction plays such a role.

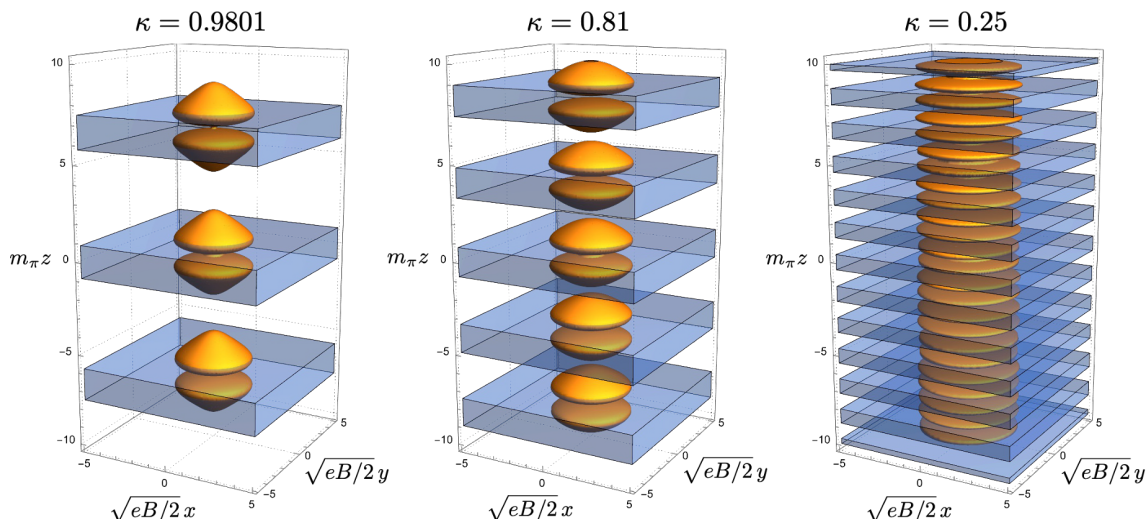


Figure 2. The minimal ($k = 1$) Skyrmion chain in the CSL with $f(w) = \sqrt{2/eB}/w$. The z coordinate is rescaled by m_π as $m_\pi z$, and the x and y coordinates are rescaled by the lump size $\sqrt{2/eB}$ as $\sqrt{2/eB}(x, y)$. The isosurface of baryon number density $\mathcal{B} = 1/(10\pi^2)$ (orange), and the sine-Gordon soliton $\pi/2 < \theta < 3\pi/2$ (blue). From the left to right panels, the elliptic modulus κ decreases ($B\mu_B$ increases) and the periodicity of the CSL decreases. The size modulus is fixed by the quantization condition, the physical width of the right configuration is smaller than that of the left configuration since smaller κ corresponds to larger B . In the rescaled coordinates, the shape changes from round (left) to crushed (right), and they look like periodic macarons (left) to a pancake tower (right).

For a single lump with $k = 1$, represented by $f = \frac{b_0}{w}$, the size and phase moduli are $|b_0|$ and arg b_0 , respectively. The relationship for n_3 is

$$n_3 = \frac{|w|^2 - |b_0|^2}{|w|^2 + |b_0|^2}, \tag{4.9}$$

and the region size D defined by $n_3 = 0$ is $|w| = |b_0|$. The flux quantization requires the size modulus to be

$$k = 1 : \quad |b_0| = \sqrt{\frac{2}{eB}}. \tag{4.10}$$

For axially symmetric k -lumps, with $f = \frac{b_0}{w^k}$, n_3 is

$$n_3 = \frac{|w|^{2k} - |b_0|^2}{|w|^{2k} + |b_0|^2}, \tag{4.11}$$

and the flux quantization requires the size modulus to be

$$|b_0| = \left(\frac{2k}{eB}\right)^{k/2}. \tag{4.12}$$

Since Skyrmons sit in the same positions (x^1, x^2) at each soliton, the total configuration in 3+1 dimensions is domain-wall Skyrmion chains. In figure 2, we plot our solutions of domain-wall Skyrmion chains for various elliptic modulus κ . The orange regions denote

the isosurface of the baryon number density $\mathcal{B} = 1/(10\pi^2)$, and the blue regions denote the soliton $\pi/2 < \theta < 3\pi/2$. One can confirm that one lump on one soliton is composed of two Skyrmions as can be expected from eq. (3.18). From the left to right panels, the elliptic modulus κ decreases corresponding to the situation that $B\mu_B$ increases, and the periodicity of the CSL decreases. From left to right, these look like from periodic macarons to a pancake tower. We note that a similar domain-wall skyrmion chain has been studied in chiral magnets in $2 + 1$ dimensions [45].

Now let us discuss a constraint from the second term of WZW term following ref. [31]. The integration of the last term in eq. (4.2) can be rewritten as

$$-\int d^2x \frac{e\mu_B}{2\pi} \epsilon^{03jk} \partial_j [A_k(1 - n_3)] = \frac{e\mu_B B}{4\pi} \oint dS_i x^i (n_3 - 1) = e\mu_B B |b_{k-1}|^2, \quad (4.13)$$

where we have used the explicit solution in eq. (4.5) in the last expression. We thus reach the energy of domain-wall Skyrmions, given by

$$E_{\text{DWSk}} = 2\pi\mathcal{C}(\kappa)|k| - 2\mu_B k + e\mu_B B |b_{k-1}|^2. \quad (4.14)$$

For a single lump ($k = 1$), we have $E_{\text{DWSk}} = 2\pi\mathcal{C}(\kappa)$ with the cancellation between the second and third terms due to the flux quantization in eq. (4.10) which is always positive. For higher winding $k \geq 2$, we have a further constraint

$$b_{k-1} = 0, \quad (4.15)$$

to minimize the domain-wall Skyrmion energy in eq. (4.14), which can become negative for sufficiently large μ_B from its second term.

Finally, let us discuss the DWSk phase in which Skyrmions are created spontaneously. From the above consideration, the phase boundary between the CSL and DWSk phases is determined to be

$$\mu_c = \pi\mathcal{C}(\kappa) = \frac{16\pi f_\pi^2 (2 - \kappa^2) E(\kappa) - 2(1 - \kappa^2) K(\kappa)}{3m_\pi \kappa^3}. \quad (4.16)$$

When $\mu_B \geq \mu_c$, the lumps have negative energy and are spontaneously created, implying the DWSk phase. Note that in the single-soliton limit $\kappa = 1$, μ_c in eq. (4.16) reduces to a constant $\frac{16\pi f_\pi^2}{3m_\pi}$ (thus a vertical line) reproducing the previous result in eq. (1.4) [31]. Since the elliptic modulus κ is determined from B and μ_B in general, eq. (4.16) gives a nontrivial curve beyond the one-soliton approximation, represented by the red curve in figure 1. This is our main result. It is interesting to observe that μ_c can be interpreted as the effective nucleon mass in this medium (inside solitons with the chemical potential μ_B and magnetic field B), which is $\frac{16\pi f_\pi^2}{3m_\pi} \sim 1.03$ GeV at the tricritical point (the white dot in figure 1), and it becomes lighter as the magnetic field is stronger.

Let us compare this boundary with the instability curve of the CSL configuration via the charged pion condensation in eq. (1.2) by Brauner and Yamamoto [12]. The full expression for the instability curve is determined by eliminating the elliptic modulus κ from

the following two equations [12]

$$\begin{aligned}
 B_{\text{CPC}} &= \frac{m_\pi^2}{\kappa^2} \sqrt{1 - \kappa^2 + \kappa^4}, \\
 \frac{E(\kappa)}{\kappa} &= \frac{e\mu_B B_{\text{CPC}}}{16\pi m_\pi f_\pi^2},
 \end{aligned}
 \tag{4.17}$$

and is denoted by the green dotted curve in figure 1. One can observe that this curve is entirely above the phase boundary between the CSL and DWSk phases in eq. (4.16), denoted by the red curve in figure 1. The CSL configuration remains locally stable (metastable) in the region between the red and green dotted curves.

Here, let us investigate the large B behaviours of these two curves. To this end, we expand the equations around $\kappa = 0$. Expanding eqs. (4.16) and (2.18) around $\kappa = 0$, we obtain

$$\mu_B \sim \frac{\pi f_\pi^2 \kappa}{2m_\pi},
 \tag{4.18}$$

$$\kappa \sim \frac{8\pi^2 m_\pi f_\pi}{\mu_B B_c},
 \tag{4.19}$$

respectively. Eliminating κ from these two equations, we obtain

$$B_c \sim \frac{4\pi^3 f_\pi^4}{\mu_B^2}.
 \tag{4.20}$$

On the other hand, expanding the instability curve of eq. (4.17) in the same way, we find that it asymptotically behaves as in eq. (1.2)

$$B_{\text{CPC}} \sim \frac{16\pi^4 f_\pi^4}{\mu_B^2} = 4\pi B_c.
 \tag{4.21}$$

Clearly, this is above the phase boundary between the CSL and DWSk phases in eq. (4.20).

5 Summary and discussion

In this paper, in the phase diagram of QCD with finite baryon density and magnetic field, we have determined the phase boundary between the CSL and DWSk phases beyond the single-soliton approximation at the leading order $\mathcal{O}(p^2)$ of ChPT. The key point to go beyond the single-soliton approximation is considering domain-wall Skyrmion chains in multiple soliton configurations. We have constructed the low-energy effective theory of one period of the CSL by the moduli approximation. We have obtained in eq. (3.31) the background-gauged $\mathbb{C}P^1$ model or $O(3)$ model with topological terms originated from the WZW term, topological lump charge in 2+1 dimensional worldvolume and the topological term for the soliton number. A single topological lump in 2+1 dimensional worldvolume theory is a superconducting ring. Due to the flux quantization condition in eq. (4.8), the size modulus is fixed. We have determined the phase boundary between the CSL and DWSk phases in eq. (4.16) denoted by the red curve in figure 1 from the negative energy condition

of the lumps. We have found that a large region in the CSL phase is occupied by the DWSk phase, and that the CSL configuration is metastable in the region between the red curve and green dotted curve given by eq. (4.17), beyond which the CSL is unstable. The blue, red and green dotted curves meet at the tricritical point in eq. (1.3).

We have worked out at the leading order $\mathcal{O}(p^2)$ of the ChPT for which we have not needed higher derivative terms such as the Skyrme term. At this order, the magnetic field is a background field. At the next leading order $\mathcal{O}(p^4)$, one needs higher derivative terms as well as the kinetic term of the electromagnetic gauge field. The stability beyond the leading order remains a future problem.

The phase transition between the CSL and DWSk phases in eq. (4.16) denoted by the red curve in figure 1 would be the so-called second order of nucleation type in the classification by de Gennes [60]. In such a case, the configuration of one side of the boundary often remains metastable on the other side, which is in fact our case. Similarly, the phase boundary between the QCD vacuum and CSL denoted by the blue curve in figure 1 was recently shown to be of the second order [22], and it should be of the nucleation type. Quantum nucleation, explored in the case of the transition from the vacuum to CSL [23, 24], should be applied to the transition from the CSL to DWSk phase. Investigating this transition is one of important future directions.

In this paper, we have obtained the periodic structure of Skyrmions: a domain-wall Skyrmion chain. Another approach is to construct an effective theory of a soliton lattice. The effective theory of each soliton is a $\mathbb{C}P^1$ model or $O(3)$ model. As was studied for a non-Abelian vortex lattice in ref. [61], we can construct a lattice effective theory as follows. A neighboring pair of solitons interacts as $H_{\text{int}} = -J \sum_{\langle i, i+1 \rangle} \mathbf{n}_i \mathbf{n}_{i+1}$ with the $\mathbb{C}P^1$ moduli \mathbf{n}_i of the i -th soliton. In our case, the lattice behaves as a ferromagnet with $J > 0$, and thus the moduli tend to be aligned. When one constructs a lump on a soliton, the system prefers to place the same lumps on its neighboring solitons. Then, that theory admits an array of lumps along the lattice direction, which is nothing but our Skyrmion chain. One can also take a continuum limit (large $B\mu_B$) resulting in a 3+1 dimensional anisotropic $\mathbb{C}P^1$ model, in which we need a careful treatment for the terms from the WZW term. Then, the continuum theory should admit a lump string along the z -direction, which should have negative energy.

Let us discuss a possible relation between our configuration of the domain-wall Skyrmion chain and an Abrikosov vortex lattice in the charged pion condensation proposed in ref. [29]. It was shown in refs. [37, 57] that when (ungauged) Skyrmions are periodically arranged with a twisted boundary condition, they reduce to global vortices in the small periodicity limit.⁴ See the rightmost panel of figure 2. In our case, these vortices should carry baryon

⁴This relation is analogous to those of periodic Yang-Mills instantons (Calorons) with a twisted boundary condition that reduce to monopoles in the same limit [62–65], and periodic $\mathbb{C}P^{N-1}$ lumps with a twisted boundary condition that reduce to $\mathbb{C}P^{N-1}$ domain walls in the same limit [53, 66, 67]. Such relations are known as a T-duality in string theory context. Moreover, these three relations are actually related to each other as follows. $SU(N)$ Yang-Mills instantons become $SU(N)$ Skyrmions [51] inside a non-Abelian domain wall [68, 69] whose worldvolume effective theory is the Skyrme model [51], and they also become $\mathbb{C}P^{N-1}$ lumps [66, 70] inside a non-Abelian vortex whose worldsheet effective theory is the $\mathbb{C}P^{N-1}$ model [71–73].

numbers [35, 74, 75]. This may offer a possible crossover between our configuration of the Skyrmion chain and an Abrikosov vortex lattice [29]. However, there is a significant difference. If we turn on a dynamical electromagnetic gauge field at the next leading order $\mathcal{O}(p^4)$, they would reduce to superconducting strings since charged pions are condensed in the vortex cores. Thus, our Skyrmion chains at the next leading order $\mathcal{O}(p^4)$ are superconducting strings in the short period limit (that is the continuum limit of the Heisenberg spin chain at large $B\mu_B$ as mentioned above).

Before concluding this paper, we wish to comment on a domain-wall Skyrmion phase analogous to the one found in QCD matter under rapid rotation [18]. Recent years have seen a surge in interest regarding rotating QCD matter [14–17, 76–86], primarily due to the observation of an exceptionally large vorticity of the order of $10^{22}/\text{s}$ in quark-gluon plasmas produced in non-central heavy-ion collision experiments at the Relativistic Heavy Ion Collider (RHIC) [87, 88]. In ChPT, the anomalous term for the η' meson was derived in [14, 15] by matching it with the chiral vortical effect (CVE) [10, 89–93] in the context of mesons. Analogous to the effect of a magnetic field, this term suggests a CSL composed of the η' meson during rapid rotation [14–16]. For two flavor scenarios, the phenomenon manifests as an η -CSL made up of the η meson. In a significant parameter region, a single η -soliton energetically decays into a couple of non-Abelian solitons, leading to neutral pion condensation in its vicinity. A lone non-Abelian soliton breaks the vector symmetry $SU(2)_V$ down to its $U(1)$ subgroup. This results in NG modes described by $SU(2)_V/U(1) \simeq \mathbb{C}P^1 \simeq S^2$, which localize near the soliton as discussed in [17]. Therefore, mirroring the π_0 soliton in a magnetic setting, each non-Abelian soliton carries $\mathbb{C}P^1$ moduli and is termed a non-Abelian sine-Gordon soliton [36, 37, 55–57]. Relying on the single-soliton approximation, we posited the DWSk phase for rapid rotations in [18]. Consequently, our present study on a domain-wall Skyrmion chain based on multiple solitons can be extended to rotational scenarios.

Acknowledgments

This work is supported in part by JSPS KAKENHI [Grants No. JP19K03839 (ME) No. JP21H01084 (KN), and No. JP22H01221 (ME and MN)] and the WPI program “Sustainability with Knotted Chiral Meta Matter (SKCM²)” at Hiroshima University (KN and MN).

Open Access. This article is distributed under the terms of the Creative Commons Attribution License ([CC-BY 4.0](https://creativecommons.org/licenses/by/4.0/)), which permits any use, distribution and reproduction in any medium, provided the original author(s) and source are credited.

References

- [1] K. Fukushima and T. Hatsuda, *The phase diagram of dense QCD*, *Rept. Prog. Phys.* **74** (2011) 014001 [[arXiv:1005.4814](https://arxiv.org/abs/1005.4814)] [[INSPIRE](#)].
- [2] S. Scherer and M.R. Schindler, *A Primer for Chiral Perturbation Theory*, Springer (2012) [[DOI:10.1007/978-3-642-19254-8](https://doi.org/10.1007/978-3-642-19254-8)] [[INSPIRE](#)].

- [3] S.K. Bogner, R.J. Furnstahl and A. Schwenk, *From low-momentum interactions to nuclear structure*, *Prog. Part. Nucl. Phys.* **65** (2010) 94 [[arXiv:0912.3688](#)] [[INSPIRE](#)].
- [4] D.T. Son and A.R. Zhitnitsky, *Quantum anomalies in dense matter*, *Phys. Rev. D* **70** (2004) 074018 [[hep-ph/0405216](#)] [[INSPIRE](#)].
- [5] D.T. Son and M.A. Stephanov, *Axial anomaly and magnetism of nuclear and quark matter*, *Phys. Rev. D* **77** (2008) 014021 [[arXiv:0710.1084](#)] [[INSPIRE](#)].
- [6] J. Goldstone and F. Wilczek, *Fractional Quantum Numbers on Solitons*, *Phys. Rev. Lett.* **47** (1981) 986 [[INSPIRE](#)].
- [7] E. Witten, *Global Aspects of Current Algebra*, *Nucl. Phys. B* **223** (1983) 422 [[INSPIRE](#)].
- [8] A. Vilenkin, *Equilibrium parity-violating current in a magnetic field*, *Phys. Rev. D* **22** (1980) 3080 [[INSPIRE](#)].
- [9] M.A. Metlitski and A.R. Zhitnitsky, *Anomalous axion interactions and topological currents in dense matter*, *Phys. Rev. D* **72** (2005) 045011 [[hep-ph/0505072](#)] [[INSPIRE](#)].
- [10] K. Landsteiner, *Notes on Anomaly Induced Transport*, *Acta Phys. Polon. B* **47** (2016) 2617 [[arXiv:1610.04413](#)] [[INSPIRE](#)].
- [11] M. Eto, K. Hashimoto and T. Hatsuda, *Ferromagnetic neutron stars: axial anomaly, dense neutron matter, and pionic wall*, *Phys. Rev. D* **88** (2013) 081701 [[arXiv:1209.4814](#)] [[INSPIRE](#)].
- [12] T. Brauner and N. Yamamoto, *Chiral Soliton Lattice and Charged Pion Condensation in Strong Magnetic Fields*, *JHEP* **04** (2017) 132 [[arXiv:1609.05213](#)] [[INSPIRE](#)].
- [13] K. Fukushima et al., *HBT signature for clustered substructures probing primordial inhomogeneity in hot and dense QCD matter*, [arXiv:2306.17619](#) [[INSPIRE](#)].
- [14] X.-G. Huang, K. Nishimura and N. Yamamoto, *Anomalous effects of dense matter under rotation*, *JHEP* **02** (2018) 069 [[arXiv:1711.02190](#)] [[INSPIRE](#)].
- [15] K. Nishimura and N. Yamamoto, *Topological term, QCD anomaly, and the η' chiral soliton lattice in rotating baryonic matter*, *JHEP* **07** (2020) 196 [[arXiv:2003.13945](#)] [[INSPIRE](#)].
- [16] H.-L. Chen, X.-G. Huang and J. Liao, *QCD phase structure under rotation*, *Lect. Notes Phys.* **987** (2021) 349 [[arXiv:2108.00586](#)] [[INSPIRE](#)].
- [17] M. Eto, K. Nishimura and M. Nitta, *Phases of rotating baryonic matter: non-Abelian chiral soliton lattices, antiferro-isospin chains, and ferri/ferromagnetic magnetization*, *JHEP* **08** (2022) 305 [[arXiv:2112.01381](#)] [[INSPIRE](#)].
- [18] M. Eto, K. Nishimura and M. Nitta, *Domain-wall Skyrmion phase in a rapidly rotating QCD matter*, [arXiv:2310.17511](#) [[INSPIRE](#)].
- [19] T. Brauner and S.V. Kadam, *Anomalous low-temperature thermodynamics of QCD in strong magnetic fields*, *JHEP* **11** (2017) 103 [[arXiv:1706.04514](#)] [[INSPIRE](#)].
- [20] T. Brauner and S. Kadam, *Anomalous electrodynamics of neutral pion matter in strong magnetic fields*, *JHEP* **03** (2017) 015 [[arXiv:1701.06793](#)] [[INSPIRE](#)].
- [21] T. Brauner, H. Kolešová and N. Yamamoto, *Chiral soliton lattice phase in warm QCD*, *Phys. Lett. B* **823** (2021) 136767 [[arXiv:2108.10044](#)] [[INSPIRE](#)].
- [22] T. Brauner and H. Kolešová, *Chiral soliton lattice at next-to-leading order*, *JHEP* **07** (2023) 163 [[arXiv:2302.06902](#)] [[INSPIRE](#)].

- [23] M. Eto and M. Nitta, *Quantum nucleation of topological solitons*, *JHEP* **09** (2022) 077 [[arXiv:2207.00211](#)] [[INSPIRE](#)].
- [24] T. Higaki, K. Kamada and K. Nishimura, *Formation of a chiral soliton lattice*, *Phys. Rev. D* **106** (2022) 096022 [[arXiv:2207.00212](#)] [[INSPIRE](#)].
- [25] Z. Qiu and M. Nitta, *Quasicrystals in QCD*, *JHEP* **05** (2023) 170 [[arXiv:2304.05089](#)] [[INSPIRE](#)].
- [26] M. Kawaguchi, Y.-L. Ma and S. Matsuzaki, *Chiral soliton lattice effect on baryonic matter from a skyrmion crystal model*, *Phys. Rev. C* **100** (2019) 025207 [[arXiv:1810.12880](#)] [[INSPIRE](#)].
- [27] S. Chen, K. Fukushima and Z. Qiu, *Skyrmions in a magnetic field and $\pi 0$ domain wall formation in dense nuclear matter*, *Phys. Rev. D* **105** (2022) L011502 [[arXiv:2104.11482](#)] [[INSPIRE](#)].
- [28] S. Chen, K. Fukushima and Z. Qiu, *Magnetic enhancement of baryon confinement modeled via a deformed Skyrmion*, *Phys. Lett. B* **843** (2023) 137992 [[arXiv:2303.04692](#)] [[INSPIRE](#)].
- [29] G.W. Evans and A. Schmitt, *Chiral anomaly induces superconducting baryon crystal*, *JHEP* **09** (2022) 192 [[arXiv:2206.01227](#)] [[INSPIRE](#)].
- [30] G.W. Evans and A. Schmitt, *Chiral Soliton Lattice turns into 3D crystal*, [arXiv:2311.03880](#) [[INSPIRE](#)].
- [31] M. Eto, K. Nishimura and M. Nitta, *How baryons appear in low-energy QCD: Domain-wall Skyrmion phase in strong magnetic fields*, [arXiv:2304.02940](#) [[INSPIRE](#)].
- [32] M. Nitta, *Correspondence between Skyrmions in 2+1 and 3+1 Dimensions*, *Phys. Rev. D* **87** (2013) 025013 [[arXiv:1210.2233](#)] [[INSPIRE](#)].
- [33] M. Nitta, *Matryoshka Skyrmions*, *Nucl. Phys. B* **872** (2013) 62 [[arXiv:1211.4916](#)] [[INSPIRE](#)].
- [34] S.B. Gudnason and M. Nitta, *Domain wall Skyrmions*, *Phys. Rev. D* **89** (2014) 085022 [[arXiv:1403.1245](#)] [[INSPIRE](#)].
- [35] S.B. Gudnason and M. Nitta, *Incarnations of Skyrmions*, *Phys. Rev. D* **90** (2014) 085007 [[arXiv:1407.7210](#)] [[INSPIRE](#)].
- [36] M. Eto and M. Nitta, *Non-Abelian Sine-Gordon Solitons: Correspondence between $SU(N)$ Skyrmions and $\mathbb{C}P^{N-1}$ Lumps*, *Phys. Rev. D* **91** (2015) 085044 [[arXiv:1501.07038](#)] [[INSPIRE](#)].
- [37] M. Nitta, *Relations among topological solitons*, *Phys. Rev. D* **105** (2022) 105006 [[arXiv:2202.03929](#)] [[INSPIRE](#)].
- [38] M. Nitta, *Josephson vortices and the Atiyah-Manton construction*, *Phys. Rev. D* **86** (2012) 125004 [[arXiv:1207.6958](#)] [[INSPIRE](#)].
- [39] M. Kobayashi and M. Nitta, *Sine-Gordon kinks on a domain wall ring*, *Phys. Rev. D* **87** (2013) 085003 [[arXiv:1302.0989](#)] [[INSPIRE](#)].
- [40] P. Jennings and P. Sutcliffe, *The dynamics of domain wall Skyrmions*, *J. Phys. A* **46** (2013) 465401 [[arXiv:1305.2869](#)] [[INSPIRE](#)].
- [41] R. Cheng et al., *Magnetic domain wall skyrmions*, *Phys. Rev. B* **99** (2019) 184412.
- [42] V.M. Kuchkin et al., *Magnetic skyrmions, chiral kinks and holomorphic functions*, *Phys. Rev. B* **102** (2020) 144422 [[arXiv:2007.06260](#)] [[INSPIRE](#)].

- [43] C. Ross and M. Nitta, *Domain-wall skyrmions in chiral magnets*, *Phys. Rev. B* **107** (2023) 024422 [[arXiv:2205.11417](#)] [[INSPIRE](#)].
- [44] Y. Amari and M. Nitta, *Chiral magnets from string theory*, *JHEP* **11** (2023) 212 [[arXiv:2307.11113](#)] [[INSPIRE](#)].
- [45] Y. Amari, C. Ross and M. Nitta, *Domain-wall skyrmion chain and domain-wall bimerons in chiral magnets*, [arXiv:2311.05174](#) [[INSPIRE](#)].
- [46] S. Lepadatu, *Emergence of transient domain wall skyrmions after ultrafast demagnetization*, *Phys. Rev. B* **102** (2020) 094402.
- [47] S.K. Kim and Y. Tserkovnyak, *Magnetic Domain Walls as Hosts of Spin Superfluids and Generators of Skyrmions*, *Phys. Rev. Lett.* **119** (2017) 047202 [[arXiv:1701.08273](#)] [[INSPIRE](#)].
- [48] S. Lee, K. Nakata, O. Tchernyshyov and S.K. Kim, *Magnon dynamics in a Skyrmion-textured domain wall of antiferromagnets*, *Phys. Rev. B* **107** (2023) 184432 [[arXiv:2211.00030](#)] [[INSPIRE](#)].
- [49] T. Nagase et al., *Observation of domain wall bimerons in chiral magnets*, *Nature Commun.* **12** (2021) 3490 [[arXiv:2004.06976](#)] [[INSPIRE](#)].
- [50] K. Yang et al., *Wigner solids of domain wall skyrmions*, *Nature Commun.* **12** (2021) 6006.
- [51] M. Eto, M. Nitta, K. Ohashi and D. Tong, *Skyrmions from instantons inside domain walls*, *Phys. Rev. Lett.* **95** (2005) 252003 [[hep-th/0508130](#)] [[INSPIRE](#)].
- [52] N.S. Manton, *A Remark on the Scattering of BPS Monopoles*, *Phys. Lett. B* **110** (1982) 54 [[INSPIRE](#)].
- [53] M. Eto et al., *Solitons in the Higgs phase: The Moduli matrix approach*, *J. Phys. A* **39** (2006) R315 [[hep-th/0602170](#)] [[INSPIRE](#)].
- [54] M. Eto et al., *Manifestly supersymmetric effective Lagrangians on BPS solitons*, *Phys. Rev. D* **73** (2006) 125008 [[hep-th/0602289](#)] [[INSPIRE](#)].
- [55] M. Nitta, *Non-Abelian Sine-Gordon Solitons*, *Nucl. Phys. B* **895** (2015) 288 [[arXiv:1412.8276](#)] [[INSPIRE](#)].
- [56] M. Nitta, *Josephson junction of non-Abelian superconductors and non-Abelian Josephson vortices*, *Nucl. Phys. B* **899** (2015) 78 [[arXiv:1502.02525](#)] [[INSPIRE](#)].
- [57] M. Nitta, *Josephson instantons and Josephson monopoles in a non-Abelian Josephson junction*, *Phys. Rev. D* **92** (2015) 045010 [[arXiv:1503.02060](#)] [[INSPIRE](#)].
- [58] A.M. Polyakov and A.A. Belavin, *Metastable States of Two-Dimensional Isotropic Ferromagnets*, *JETP Lett.* **22** (1975) 245 [[INSPIRE](#)].
- [59] C. Ross, N. Sakai and M. Nitta, *Skyrmion interactions and lattices in chiral magnets: analytical results*, *JHEP* **02** (2021) 095 [[arXiv:2003.07147](#)] [[INSPIRE](#)].
- [60] P.G. de Gennes, *Phase Transition and Turbulence: An Introduction*, Springer US, Boston, MA, U.S.A. (1975), p. 1–18 [[DOI:10.1007/978-1-4615-8912-9_1](#)].
- [61] M. Kobayashi, E. Nakano and M. Nitta, *Color Magnetism in Non-Abelian Vortex Matter*, *JHEP* **06** (2014) 130 [[arXiv:1311.2399](#)] [[INSPIRE](#)].
- [62] K.-M. Lee, *Instantons and magnetic monopoles on $R^3 \times S^1$ with arbitrary simple gauge groups*, *Phys. Lett. B* **426** (1998) 323 [[hep-th/9802012](#)] [[INSPIRE](#)].

- [63] K.-M. Lee and C.-H. Lu, *SU(2) calorons and magnetic monopoles*, *Phys. Rev. D* **58** (1998) 025011 [[hep-th/9802108](#)] [[INSPIRE](#)].
- [64] T.C. Kraan and P. van Baal, *Periodic instantons with nontrivial holonomy*, *Nucl. Phys. B* **533** (1998) 627 [[hep-th/9805168](#)] [[INSPIRE](#)].
- [65] T.C. Kraan and P. van Baal, *Monopole constituents inside SU(n) calorons*, *Phys. Lett. B* **435** (1998) 389 [[hep-th/9806034](#)] [[INSPIRE](#)].
- [66] M. Eto et al., *Instantons in the Higgs phase*, *Phys. Rev. D* **72** (2005) 025011 [[hep-th/0412048](#)] [[INSPIRE](#)].
- [67] M. Eto et al., *Non-Abelian vortices on cylinder: Duality between vortices and walls*, *Phys. Rev. D* **73** (2006) 085008 [[hep-th/0601181](#)] [[INSPIRE](#)].
- [68] M. Shifman and A. Yung, *Localization of nonAbelian gauge fields on domain walls at weak coupling (D-brane prototypes II)*, *Phys. Rev. D* **70** (2004) 025013 [[hep-th/0312257](#)] [[INSPIRE](#)].
- [69] M. Eto et al., *Domain walls with non-Abelian clouds*, *Phys. Rev. D* **77** (2008) 125008 [[arXiv:0802.3135](#)] [[INSPIRE](#)].
- [70] A. Hanany and D. Tong, *Vortex strings and four-dimensional gauge dynamics*, *JHEP* **04** (2004) 066 [[hep-th/0403158](#)] [[INSPIRE](#)].
- [71] A. Hanany and D. Tong, *Vortices, instantons and branes*, *JHEP* **07** (2003) 037 [[hep-th/0306150](#)] [[INSPIRE](#)].
- [72] R. Auzzi et al., *NonAbelian superconductors: Vortices and confinement in N = 2 SQCD*, *Nucl. Phys. B* **673** (2003) 187 [[hep-th/0307287](#)] [[INSPIRE](#)].
- [73] M. Eto et al., *Moduli space of non-Abelian vortices*, *Phys. Rev. Lett.* **96** (2006) 161601 [[hep-th/0511088](#)] [[INSPIRE](#)].
- [74] S.B. Gudnason and M. Nitta, *Skyrmions confined as beads on a vortex ring*, *Phys. Rev. D* **94** (2016) 025008 [[arXiv:1606.00336](#)] [[INSPIRE](#)].
- [75] M. Nitta, *Fractional instantons and bions in the principal chiral model on $\mathbb{R}^2 \times S^1$ with twisted boundary conditions*, *JHEP* **08** (2015) 063 [[arXiv:1503.06336](#)] [[INSPIRE](#)].
- [76] H.-L. Chen, K. Fukushima, X.-G. Huang and K. Mameda, *Analogy between rotation and density for Dirac fermions in a magnetic field*, *Phys. Rev. D* **93** (2016) 104052 [[arXiv:1512.08974](#)] [[INSPIRE](#)].
- [77] S. Ebihara, K. Fukushima and K. Mameda, *Boundary effects and gapped dispersion in rotating fermionic matter*, *Phys. Lett. B* **764** (2017) 94 [[arXiv:1608.00336](#)] [[INSPIRE](#)].
- [78] Y. Jiang and J. Liao, *Pairing Phase Transitions of Matter under Rotation*, *Phys. Rev. Lett.* **117** (2016) 192302 [[arXiv:1606.03808](#)] [[INSPIRE](#)].
- [79] M.N. Chernodub and S. Gongyo, *Interacting fermions in rotation: chiral symmetry restoration, moment of inertia and thermodynamics*, *JHEP* **01** (2017) 136 [[arXiv:1611.02598](#)] [[INSPIRE](#)].
- [80] M.N. Chernodub and S. Gongyo, *Effects of rotation and boundaries on chiral symmetry breaking of relativistic fermions*, *Phys. Rev. D* **95** (2017) 096006 [[arXiv:1702.08266](#)] [[INSPIRE](#)].
- [81] Y. Liu and I. Zahed, *Rotating Dirac fermions in a magnetic field in 1+2 and 1+3 dimensions*, *Phys. Rev. D* **98** (2018) 014017 [[arXiv:1710.02895](#)] [[INSPIRE](#)].

- [82] H. Zhang, D. Hou and J. Liao, *Mesonic Condensation in Isospin Matter under Rotation*, *Chin. Phys. C* **44** (2020) 111001 [[arXiv:1812.11787](#)] [[INSPIRE](#)].
- [83] L. Wang, Y. Jiang, L. He and P. Zhuang, *Local suppression and enhancement of the pairing condensate under rotation*, *Phys. Rev. C* **100** (2019) 034902 [[arXiv:1901.00804](#)] [[INSPIRE](#)].
- [84] H.-L. Chen, X.-G. Huang and K. Mameda, *Do charged pions condense in a magnetic field with rotation?*, [arXiv:1910.02700](#) [[INSPIRE](#)].
- [85] M.N. Chernodub, *Inhomogeneous confining-deconfining phases in rotating plasmas*, *Phys. Rev. D* **103** (2021) 054027 [[arXiv:2012.04924](#)] [[INSPIRE](#)].
- [86] M.N. Chernodub, V.A. Goy and A.V. Molochkov, *Inhomogeneity of a rotating gluon plasma and the Tolman-Ehrenfest law in imaginary time: Lattice results for fast imaginary rotation*, *Phys. Rev. D* **107** (2023) 114502 [[arXiv:2209.15534](#)] [[INSPIRE](#)].
- [87] STAR collaboration, *Global Λ hyperon polarization in nuclear collisions: evidence for the most vortical fluid*, *Nature* **548** (2017) 62 [[arXiv:1701.06657](#)] [[INSPIRE](#)].
- [88] STAR collaboration, *Global polarization of Λ hyperons in Au+Au collisions at $\sqrt{s_{NN}} = 200$ GeV*, *Phys. Rev. C* **98** (2018) 014910 [[arXiv:1805.04400](#)] [[INSPIRE](#)].
- [89] A. Vilenkin, *Macroscopic parity-violating effects: Neutrino fluxes from rotating black holes and in rotating thermal radiation*, *Phys. Rev. D* **20** (1979) 1807 [[INSPIRE](#)].
- [90] A. Vilenkin, *Quantum field theory at finite temperature in a rotating system*, *Phys. Rev. D* **21** (1980) 2260 [[INSPIRE](#)].
- [91] D.T. Son and P. Surowka, *Hydrodynamics with Triangle Anomalies*, *Phys. Rev. Lett.* **103** (2009) 191601 [[arXiv:0906.5044](#)] [[INSPIRE](#)].
- [92] K. Landsteiner, E. Megias and F. Pena-Benitez, *Gravitational Anomaly and Transport*, *Phys. Rev. Lett.* **107** (2011) 021601 [[arXiv:1103.5006](#)] [[INSPIRE](#)].
- [93] K. Landsteiner, E. Megias and F. Pena-Benitez, *Anomalous Transport from Kubo Formulae*, *Lect. Notes Phys.* **871** (2013) 433 [[arXiv:1207.5808](#)] [[INSPIRE](#)].